

**Supplementary Material for
“Synergistic chromatin-modifying treatments reactivate latent HIV and decrease
migration of multiple host-cell types”**

Alexandra Blanco, Tarun Mahajan, Robert A. Coronado, Kelly Ma, Dominic R. Demma,
and Roy D. Dar*

*Corresponding author. Email: roydar@illinois.edu

Contents:

Figures S1 – S7	(Pages 2-8)
Tables S1 – S2	(Page 9)
References	(Page 10)

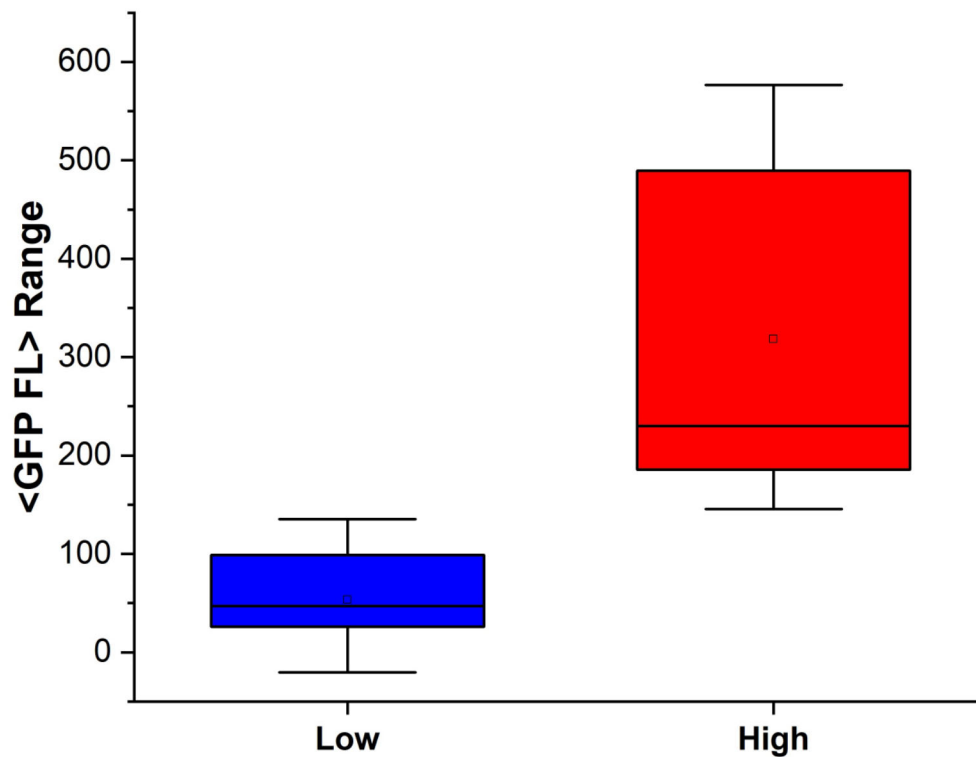


Figure S1. Distribution of THP-1 Ld2G clonal library. A library of 35 THP-1 Ld2G clonal cell lines was generated and separated into two differentially expressed categories (high and low) according to the GFP fluorescence expressed from each clonal population. A clone was randomly selected from each of the high/low expression categories to test synergistic over-expression of the HIV LTR promoter in THP-1 monocytes for two different integration sites. Each box is determined by the 25th and 75th percentiles. The whiskers are determined by the 5th and 95th percentiles. The horizontal line within each box represents the median, and the open circle represents the mean.

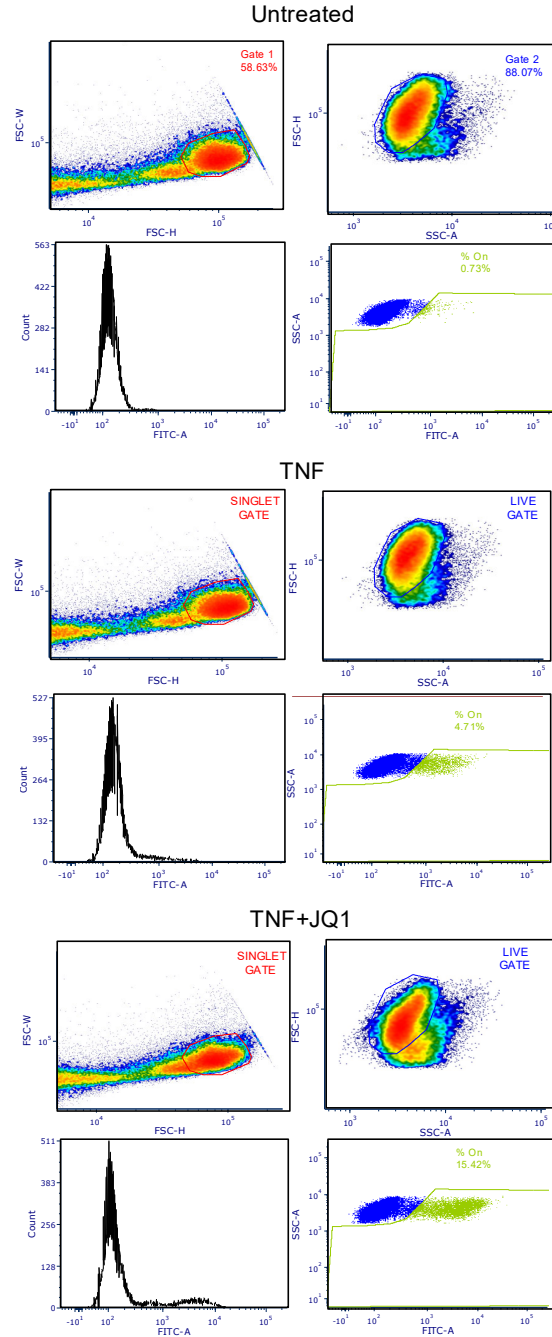


Figure S2. Flow cytometry gating strategy for TLat 2C8 reactivation measurements. A 3-layer nested gating was employed to gauge the reactivation percentage of the TLat. The top panel shows the untreated sample, while the middle and lower panels show samples treated with TNF, and TNF+JQ1, respectively. The hierarchy for the 3-layer gating is as follows: the top layer, shown as the “singlet” gate in red, filters out single events that consist of two independent particles. The middle layer, shown as the “live” gate in blue, excludes debris and dead cells. The bottom layer, shown as “% On” in green, includes cells with higher fluorescence than the untreated autofluorescence. Cells that fall in this gate represent the reactivation percentage of the population.

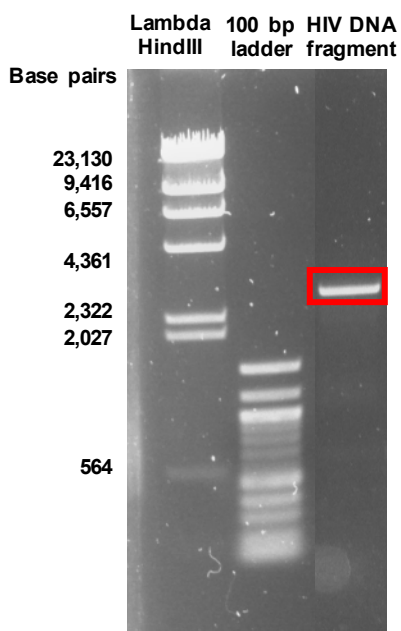


Figure S3. Detection of HIV DNA in TLat 2C8. As a control, to confirm the presence of HIV DNA in the generated TLat 2C8, a ~2.9 kbp fragment of the *gag* gene was amplified via PCR. The resulting amplified fragment was run on an agarose gel, stained with SYBR green, and imaged using blue light. The amplified fragment is of correct size, as visualized by comparison with the DNA marker.

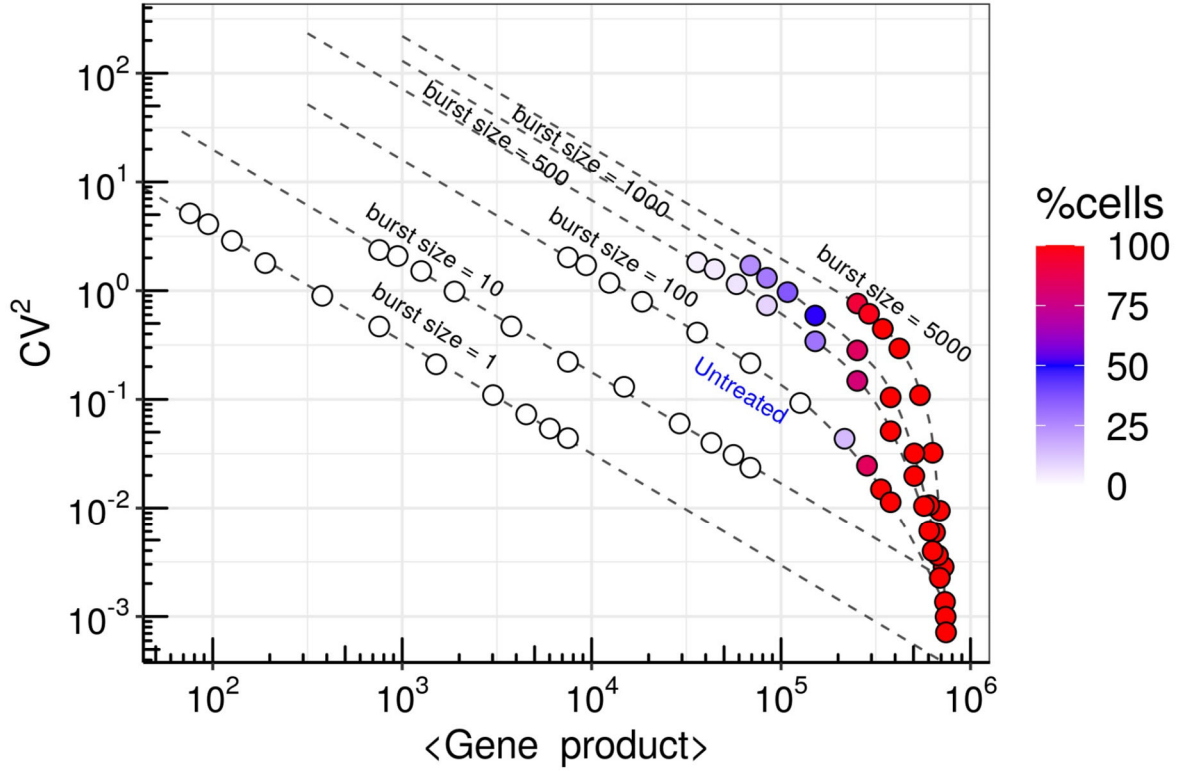


Figure S4. Noise-vs-mean map. Noise (CV^2)-vs-mean map for different combinations of burst size and frequency for the two-state model of transcriptional bursting for the LTR promoter. Each sphere in the plot represents steady-state mean and noise values calculated from 1000 different single-cells for a specific combination of burst size and frequency. Iso-burst lines are marked with dashed lines. For each iso-burst line, the same set of burst frequencies were simulated. As the burst size increases, the burst frequency at which reactivation starts decreases. For high enough burst size, as burst frequency increases, % of cells which cross the active replication threshold also increases. The set of burst sizes and frequencies which were used are given in Table S2. Burst size was modulated by varying k_{off} , while burst frequency was modulated by varying k_{on} . “Untreated” denotes the simulated burst size and frequency used in Figure 1C.

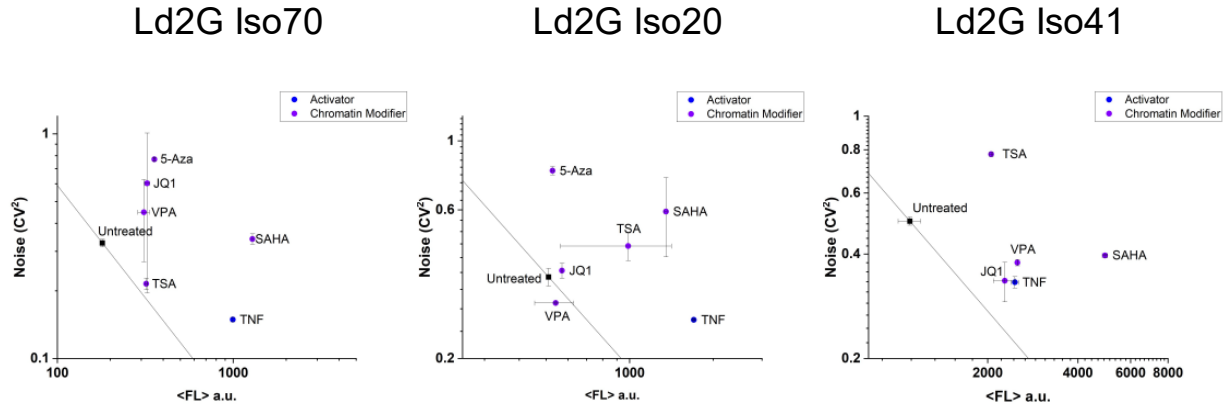


Figure S5. Noise-mean quantification for three Jurkat Ld2G isoclonal cell lines under diverse treatments. For isoclonal cell lines 70 and 20, in general, chromatin modifying treatments increase transcriptional burst size and decrease burst frequency, while TNF increases both transcriptional burst size and frequency. For the highly-expressed integration site (Iso41), except for TSA treatment, chromatin modifiers (purple) appear to increase mean by increasing burst frequency with increasing burst size.

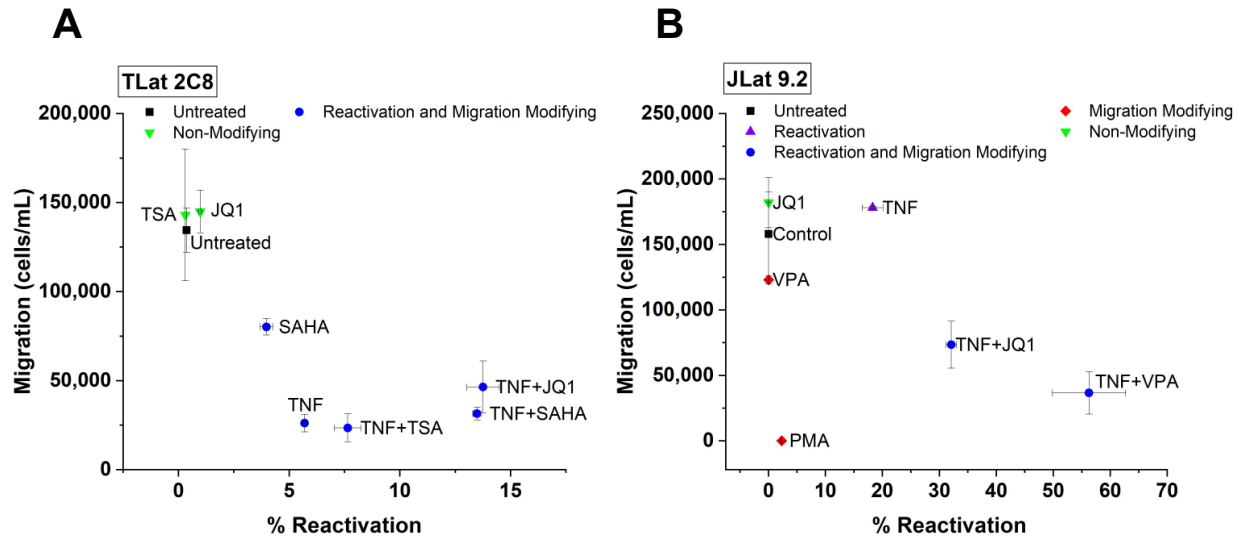


Figure S6. LRA Cocktails Affect Reactivation and Cell Migration. LRA treatments affect cell migration and latent reactivation in TLat 2C8 (Left) and JLat 9.2 (Right) at different levels. In both monocytes and T-cells, synergistic LRA cocktails decrease cell migration. TSA and JQ1 alone do not seem to affect migration, while VPA reduces T-cell migration and SAHA reduces monocyte migration in addition to providing some reactivation. TNF affects only reactivation in T-cells, but appears to affect both reactivation and migration in monocytes. Consistent with reported literature [1], PMA, a PKC agonist, completely internalizes CXCR4 from the cell surface in T-cells, resulting in no cell migration (and no CXCR4 staining on the surface). Experiments were performed in duplicate or triplicate and mean and standard error were plotted.

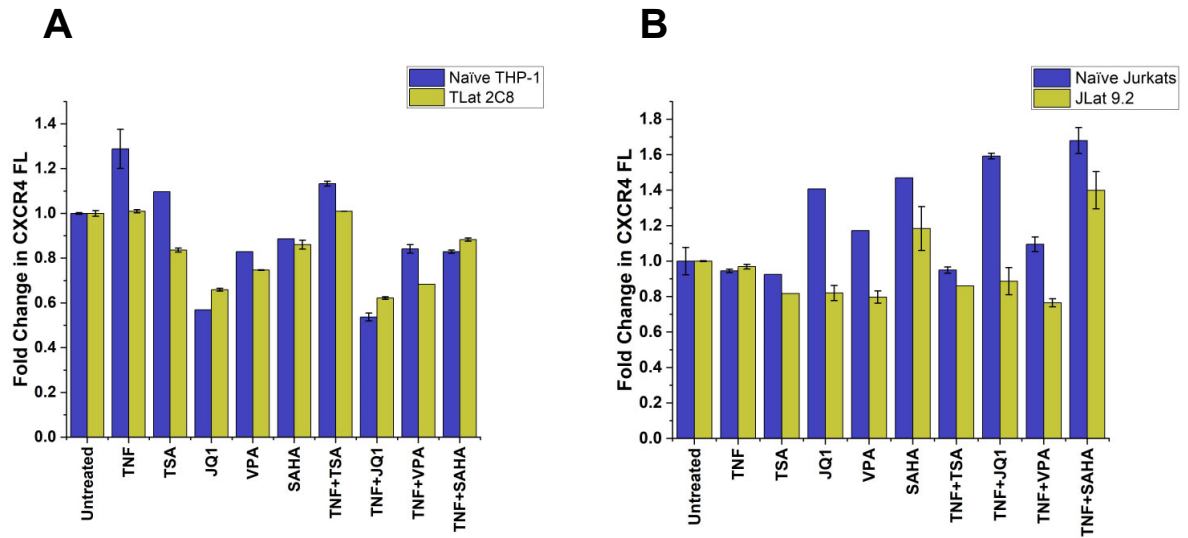


Figure S7. LRA treatment and viral reactivation affect CXCR4 surface expression.

Latently-infected and naïve (uninfected) THP-1 monocytes (Left) and Jurkats (Right) were treated with LRAs for 24h to monitor fold change (F.C.) in CXCR4 surface expression of treated to untreated cells. LRAs affect CXCR4 surface expression as shown by changes in CXCR4 fluorescence (FL) in naïve cells. In the context of T-cell JLat 9.2 reactivation (right panel), we see that this F.C. is further reduced, showing that latent reactivation, in addition to LRA treatment, can modify CXCR4 surface expression levels. This effect is more pronounced in Jurkat T-cells than in THP-1 monocytes. Since monocytes have lower surface expression of CXCR4 (Figure 4) [2, 3], major differences in F.C. due to viral reactivation appear difficult to resolve, and it appears like both uninfected and infected cells are dominated by the LRA treatment effect (left panel).

Table S1. Simulation parameters for Fig. 1C. Parameters also used in [4].

Simulation Parameter	Biological Interpretation	UN Simulation	NE Simulation	AC Simulation	AC+NE Simulation
k_{on}	Initiation rate	0.000208333 sec-1	0.000104167 sec-1	0.000625 sec-1	0.000625 sec-1
k_{off}	OFF rate	0.002083333 sec-1	0.001041667 sec-1	0.002083 sec-1	0.001041667 sec-1
k_m	Expression rate	0.208333333 sec-1	0.208333333 sec-1	0.208333333 sec-1	0.208333333 sec-1
γ_m	mRNA degradation rate	0.000115525 sec-1	0.000115525 sec-1	0.000115525 sec-1	0.000115525 sec-1
k_p	Translation rate	0.032346868 sec-1	0.032346868 sec-1	0.032346868 sec-1	0.032346868 sec-1
γ_p	Protein degradation rate	7.70164E-05 sec-1	7.70164E-05 sec-1	7.70164E-05 sec-1	7.70164E-05 sec-1

Table S2. Burst size and frequency values used in Fig. 1D. k_{on} is the burst frequency for untreated in Fig. 1C.

Burst Size	Burst Frequency ($k_{on}/k_{on, UN}$)
1	1/10
10	1/8
50	1/6
100	1/4
500	1/2
1000	1
5000	2
	4
	6
	8
	10

References

1. Clift, I.C., et al., *β -Arrestin1 and Distinct CXCR4 Structures Are Required for Stromal Derived Factor-1 to Downregulate CXCR4 Cell-Surface Levels in Neuroblastoma*. *Molecular Pharmacology*, 2014. **85**(4): p. 542-552.
2. Gupta, S.K., K. Pillarisetti, and P.G. Lysko, *Modulation of CXCR4 expression and SDF-1 α functional activity during differentiation of human monocytes and macrophages*. *Journal of leukocyte biology*, 1999. **66**(1): p. 135-143.
3. Cassol, E., et al., *Monocyte-derived macrophages and myeloid cell lines as targets of HIV-1 replication and persistence*. *Journal of Leukocyte Biology*, 2006. **80**(5): p. 1018-1030.
4. Dar, R.D., et al., *Screening for noise in gene expression identifies drug synergies*. *Science*, 2014. **344**(6190): p. 1392-1396.